Available online at www.sciencedirect.com

SciVerse ScienceDirect

Procedia CIRP 5 (2013) 253 – 258

www.elsevier.com/locate/procedia

The First CIRP Conference on Biomanufacturing

Adaptable Orthopedic Shape Memory Implants

Ronny Pfeifer[a]*, Christian W. Müller[b], Christof Hurschler[c], Stefan Kaierle[a], Volker Wesling[a], Heinz Haferkamp[a]

[a]*Laser Zentrum Hannover e.V., Hollerithallee 8, 30419 Hannover, Germany*
[b]*Trauma Department, Hannover Medical School (MHH), Carl-Neuberg-Str. 4, 30176 Hannover, Germany*
[c]*Laboratory for Biomechanics and Biomaterials, Department of Orthopaedics, Hannover Medical School (MHH), Anna-von-Borries-Str. 1-7, 30625 Hannover, Germany*

* Corresponding author. Tel.: +49-511-2788-161; fax: +49-511-2788-100. *E-mail address*: r.pfeifer@lzh.de

Abstract

Apart from biological factors, the bone healing process strongly depends on the mechanical properties of the implant applied. The stiffness of the implant influences the micro-motion, one of the most important stimuli of the healing process within the fracture gap. Both, the "ideal" stiffness of an implant as well as the alteration of the mechanical properties over the course of healing are still a topic of research. Apart from biodegradable implants or "fixateur externe", it is not possible to alter the mechanical properties of the implants without second surgery. A "stiffness alterable" implant might have a positive impact on the healing process, e.g. a shorter healing time, an early ability to bear weight or the avoidance of a follow-on operation.
In order to adapt the implant to the actual healing situation, nickel-titanium (NiTi) shape memory alloy (SMA) based implants that exhibit a variable middle piece were developed. Due to contactless induction heating, the transition temperature of the SMA is reached and triggers the one-way shape memory effect (SME). This leads to a slight modification of the second moment of inertia and to an adaption of the bending stiffness of the implant, respectively. Based on laser cutting and welding, NiTi-SMA based implants were manufactured by using thin, commercially available NiTi (thickness: 0.5 and 1.0 mm, transition temperature A_f between 55-65°C) sheets. Depending on the implant design, 4-Point-Bending measurements showed feasible bending stiffness alterations around a range of 50 %, with regard to the original stiffness. Thereby, two approaches, increasing the bending stiffness and decreasing the bending stiffness, have been realized.
Currently, the implant design is being adapted in order to meet the requirements for human applications. Custom made NiTi-SMA with a transition temperature around 45-50°C could continue to reduce the impact of the heating process and expand this concept to further medical applications, e.g. compression, anchoring or expansion of implants or devices.

Keywords: implant; bone; stiffness; NiTi; Nitinol; SMA; SME; shape memory; laser

1. Introduction

Since the first application of a nickel-plated steel implant to join bone fragments after a fracture by Carl Hansmann in 1886, both the implant materials and the functionality (design, locking principle, etc.) have been continuously improved [1]. Besides conventional compression plates allowing for a direct connection between the fragments (primary bone healing), a multitude of today´s implants lead to a "natural" healing process (secondary bone healing) under formation of a stabilizing callus [2]. As this process is strongly related to a relative (interfragmentary) motion of the bone fragments [3], a possible alteration of the implant´s bending stiffness could have a direct impact on the bone healing process [4]. According to Wolff´s law [5], the reduction of the stiffness of an implant in the same degree as the bone is able to bear load again during the healing process, could facilitate the bone healing

2212-8271 © 2013 The Authors. Published by Elsevier B.V. Open access under CC BY-NC-ND license.
Selection and/or peer-review under responsibility of Professor Mamoru Mitsuishi and Professor Paulo Bartolo
doi:10.1016/j.procir.2013.01.050

process. However, apart from biodegradable implants or a “fixateur externe”, an alteration of the mechanical properties of the stabilizing component (if necessary) requires an additional surgery.

Using shape memory alloys as implant material, offering the possibility to alter the stiffness of the implants at a particular time, could therefore improve the bone healing process in terms of healing time, stability or a decreased rate of non-union.

This article shows the development of NiTi based implants with adaptable bending stiffness. After laser cutting of the NiTi-SMA segments [6], the implants were manufactured by laser welding and slight manual mechanical deformation of the centered actuator part (cf. Fig. 3 and 6). After implantation, the one-way SME is triggered using an induction device inducing a slight geometric modification within the (deformed) actuator part of the implant [7, 8]. In order to prove the general principle, a stiffness alteration in both directions (increase [9] and decrease) was investigated.

1.1. NiTi-SMAs for medical applications

Based on its outstanding properties (one-way-, two-way-shape memory effect, pseudoplasticity) and its excellent biocompatibility [10], NiTi-SMAs (nearly equiatomic intermetallic compound containing 54-60 wt% Ni, rest Ti) are the most common SMAs in medicine [11, 12, 13].

Compared to other metallic alloys exhibiting the SME (e.g. CuAlNi, CuZnAl, Fe-based alloys), they offer the most pronounced one- and two-way SME, a high mechanical strength and a high efficiency in converting thermal in mechanical energy [14]. Several physical and mechanical properties are shown in Tab. 1.

Table 1. Selected physical and mechanical properties of common metallic SMAs [14, 15].

	Unit	NiTi	CuZnAl	CuAlNi
Fusion point	°C	1250	1050	1020
Density	g/cm³	6.4-6.5	7.5-8.0	7.1-7.2
Specific heat	J/kg K	490	440	390
Young´s modulus	GPa	23-83	80-100	70-100
Yield strength	MPa	100-130	70	40
Tensile strength	MPa	875	800	700
Corrosion resistance		excellent	good	average
Biocompatibility		excellent	poor	poor

Currently, NiTi-SMAs are clinically applied as stents in cardiovascular surgery [16], guide wires for catheters, filters [17], or wires for orthodontic uses [18]. In the orthopedic field they are used as staples for foot or hand surgery, for example [19, 20]. Several studies were carried out in order to expand the field of applications, e.g. the use of NiTi staples to treat radius fractures [21] or as stent for colon obstruction [22].

1.2. One-way shape memory effect

The one-way SME is based on a reversible martensitic phase transformation (Fig. 1, top). Below the martensit-finish-temperature M_f, the NiTi-SMA shows a twinned martensitic structure. This phase can be easily mechanically deformed. Depending on the structure and the thermomechanical treatment, NiTi-SMAs offer a maximum reversible strain of 6-8 % [23, 24]. By increasing the temperature above the austenite-start-temperature A_s the martensite converts into austenite, engaging the original geometrical shape, simultaneously (Fig. 1, bottom).

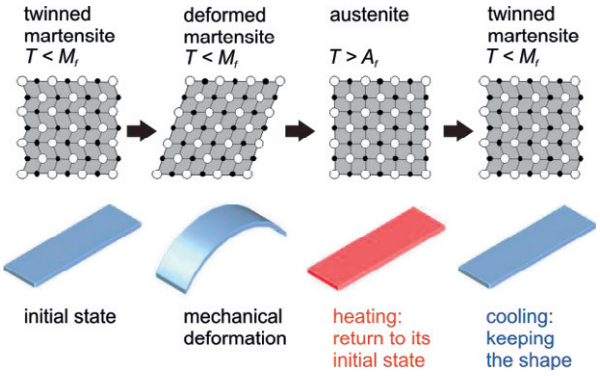

Fig. 1. Schematic illustration of the microscopic (top) and macroscopic (bottom) one-way shape memory effect.

This process is completed when reaching the austenite-finish-temperature A_f, as the NiTi-SMA is now fully austenitic (cf. Fig. 2). Cooling down, beginning at the martensite-start-temperature M_s, the austenite converts into twinned martensite again, while keeping the shape. Below M_f the reconversion into twinned martensite is completed [11].

As the transition temperatures can be adjusted by altering the alloy composition ($\Delta T \approx 10$ K when changing the composition about 0.1 at%), it is possible to fabricate NiTi-alloys for very different applications, in terms of the particular transition temperature.

It should be noted that the conversion into austenite and reconversion into martensite underlie a hysteresis, which typically amounts to 20-40 K (Fig. 2).

1.3. Laser processing

NiTi-SMAs are very sensitive to stress, thermal influences and mechanical tensions. Due to the low Young´s modulus, the high ductility and the low thermal

conductivity, mechanical machining is very difficult and results in increased tool wear and in degradation of the machined surface [25].

Laser processing, characterized by a precise localized non-contact energy input, allows both, cutting and welding with a high quality, a small heat affected zone (HAZ) and a fast machining speed. Hence, it offers an ideal method for the processing of NiTi-SMA.

1.4. Theoretical viewing

The bending stiffness k (N/mm^4) is related to the Young´s modulus E (GPa) and the second moment of inertia I (mm^4).

While E is usually specific for the material, NiTi-SMA can nearly double its Young´s modulus ($E_{martensite}$ = 23-41 GPa, $E_{austenite}$ = 70-83 GPa) depending on its state, i.e. on its temperature [15]. With regard to the NiTi-SMA-implant, based on the transition temperature of the alloy, three different scenarios are possible (Fig. 2). If the ambient (body) temperature T_b is lower or equal to M_f, the Young´s modulus remains the same before and after inducing the one-way SME (Fig. 2, S_1). In contrast, if $M_f \leq T_b \leq A_s$ (Fig. 2, S_2), only partial reconversion (austenite into martensite) may occur. Hence the Young´s modulus increases compared to the original state. In scenario three (Fig. 2, S_3), i.e. T_b is higher than A_s (or A_f, respectively), the SME would directly be triggered while implantation, and is therefore not considered for this application. However, exactly this scenario is used for NiTi staples in foot or hand surgery (alloy B, $A_f \leq 37$°C) as the staples are inserted in cooled condition and "activated" by the body temperature [19, 20].

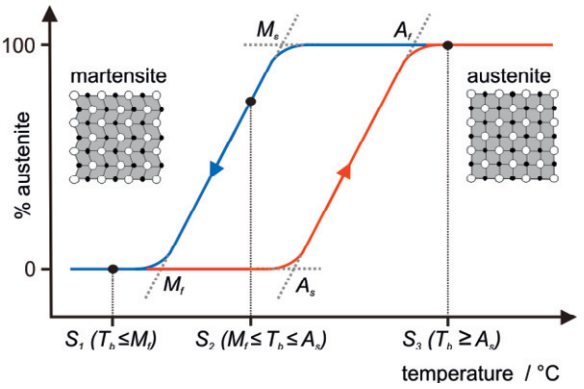

Fig. 2. Schematic illustration of the phase transformation and the hysteresis of NiTi-SMAs.

Beside the alteration of the Young´s modulus, the more interesting possibility to alter the bending stiffness is the adaption of the second moment of inertia (Fig. 3). Based on the one-way-SME, the geometry of the cross-section is modified. Advantageously, based on the design, the second moment of inertia can be either in- or decreased, hence the bending stiffness of the implant can be raised or reduced (cf. Fig. 6).

Combining these two effects allows a high rate of adaption of the bending stiffness. However, as a matter of principle, the alteration (increase) of the Young´s modulus is only helpful when a raise of the bending stiffness is intended. When decreasing the bending stiffness, the implant has to be fully martensitic at body temperature, otherwise the increased Young´s modulus would reduce or compensate, respectively, the lowered second moment of inertia.

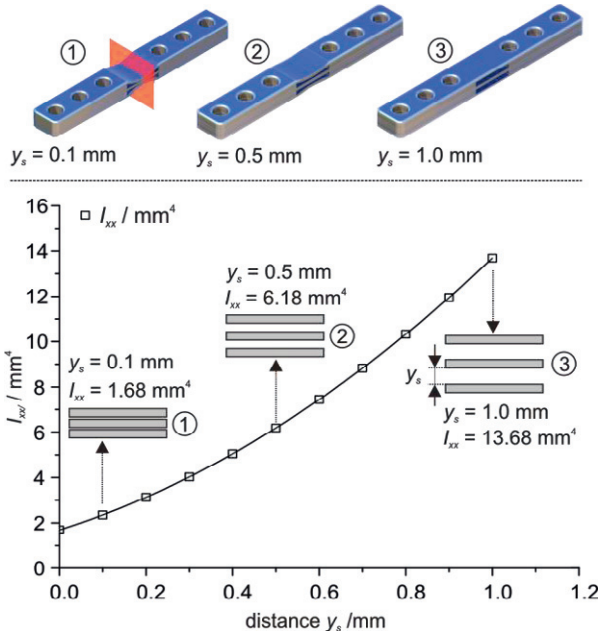

Fig. 3. General principle to adapt the bending stiffness (here: increase) of the NiTi-SMA implant by changing the geometry of the inner part of the implant (top). The diagram (bottom) shows the cross section related to the actual state of the implant. Furthermore the second moment of inertia, depending on the distances of the NiTi-SMA sheets is depicted.

2. Materials and Methods

2.1. NiTi-shape memory alloy

Polycrystalline NiTi sheets (alloy M, Memry GmbH, Germany) with a thickness of 0.5 and 1.0 mm were used as raw material. After cold rolling, the sheets were flat annealed and chemically etched in order to remove the oxide layer. DSC measurements (T_{min} = -20°C, T_{max} = 110°C, heating-up/cooling-down rate: 10 K/min) showed a A_s of 50.8°C and a A_f of 63.0°C.

2.2. Laser set-up

To cut the SMA-segments out of the sheets, a pulsed Nd:YAG laser (FLS 352 N, LASAG AG, Switzerland, $\lambda = 1064$ nm) was employed. Instead of nitrogen, argon was used as process gas in order to avoid nitriding and the resulting additional heating of the cutting edge.

After cutting, the NiTi segments were welded together under inert gas (argon) atmosphere ($c_{o2} < 100$ ppm). As for small implants samples only a small welding depth was necessary, a pulsed laser was used (Trumpf TruPulse 103, Germany, $\lambda = 1064$ nm). Bigger implant samples were manufactured using a continuous-wave (cw) disc laser (Trumpf TruDisc 16002, Germany, $\lambda = 1070$ nm), allowing for a higher welding depth.

2.3. Four-Point-Bending Measurement

In order to determine the bending stiffness of the NiTi-SMA implants, a four-point bending test was performed (Mini Bionix 858, MTS Systems, Minneapolis, USA) according to ISO 9585: 1990(E). A water filled PMMA chamber, surrounding the testing rig, allowed inducing the one-way SME. Therefore the water was heated up to A_f using a thermostat/pumping device (CC-205, Huber, Offenburg, Germany) [9].

3. Results and Discussion

3.1. Laser processing

In order to remain the shape-memory properties and to minimize the thermal impact on the SMA, suitable laser and process parameters were determined. Using a pulse frequency (f) of 100 Hz and a pulse energy of 0.3-1.0 J (pulse duration 0.15-1.5 ms) small kerf widths (150-300 µm) and a small angle of taper (< 2°) were achieved [6]. Compared to short- and ultrashort laser processing, deploying almost no thermal impact [26-28], an increased heat-affected zone (up to 30 µm) and a higher roughness (R_z = 10-30 µm) were determined [6].

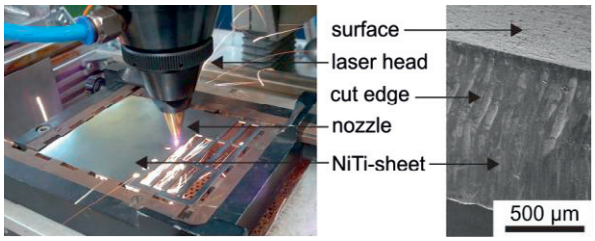

Fig. 4. Pulsed Nd:YAG laser cutting of 1 mm NiTi-SMA sheets (left). Exemplary SEM picture of the cut surface after the cutting process (pulse duration = 1.0 ms, pulse energy = 0.8 J, processing speed $v = 3.3$ m/s, $f = 100$ Hz) [6].

However, compared to short- and ultrashort laser processing, this process also allows for a higher cutting speed (up to 12 mm/s) and the possibility to machine macro-SMA components (thickness: mm-range) [6]. In terms of the cut-quality and the cutting speed, the pulsed Nd:YAG laser cutting offers a suitable method to generate macroscopic NiTi samples.

After cutting, the individual segments were clamped and welded together (Fig. 5, left) using a pulsed laser process. An exemplary cross-section of an overlap seam, generated by pulsed laser process, is shown in the middle of Fig. 5 (welding depth ≈ 0.7 mm). The weld zone is marked by red dots, whereas the HAZ is marked by white dots. It can be seen, that the seam is wide at the top, compared to the welding depth.

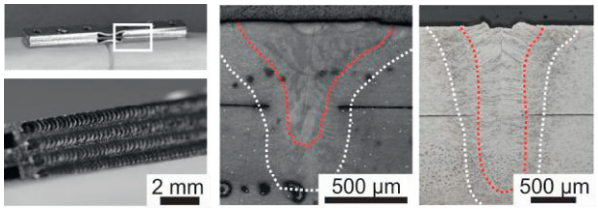

Fig. 5. NiTi-SMA implant samples. Left: Implant sample (top) and a enlarged viewing of the weld seams (bottom). Middle: cross-section of weld seam generated by pulsed laser welding (pulse energy = 6 J, pulse duration = 3 ms, $f = 10$ Hz, overlap: 75%). Right: cross-section of weld seam generated by cw laser welding (laser power = 1.5 kW, v =6.0 m/min).

The short laser pulses allow for a very controllable and minimized heat impact. Hence, the overall temperature and therefore the distortion can be kept very low. Thus, even pre-deformed NiTi segments can be welded without triggering the one-way SME. However, using a pulsed laser welding process, the achievable welding depth is in range of only a few millimeter, which is sufficient for the small implant samples but not for implants with a bigger size.

In order to achieve a higher welding depth, a continuous-wave welding process was deployed. Fig. 5 (right) shows an exemplary cross-section of an overlap weld seam, generated by a cw-process. Compared to the cross-section generated by pulsed laser welding, a narrow and even weld zone is achieved.

Despite the low seam width at the top, a high welding depth can be achieved (deep/key-hole-welding process). Using a laser power of 1.5 kW ($v = 2$ m / min) an aspect ratio (depth to width) of up to 5.4:1 (welding depth: 3.8 mm) was determined, allowing to weld implants with bigger dimensions.

Compared to the pulsed welding process, a welding speed of at least one order of magnitude higher was realized. However, due to the higher heat impact, the implant is heated above A_f, hence the one-way SME is

triggered during the welding process. Consequently, the implant design has to enable a deformation after welding.

Fig. 6 shows two different implant samples, generated by laser cutting and welding (l x w x h: 53 x 6 x 3.5 mm³ (left), 53 x 8 x 3.5 mm³ (right)). Triggering the one-way-SME results in straightening of the outer sheets in the middle, actuator part of the implant. Whereas the second moment of inertia of the left implant is increased, straightening of the right implant results in a decreased second moment of inertia.

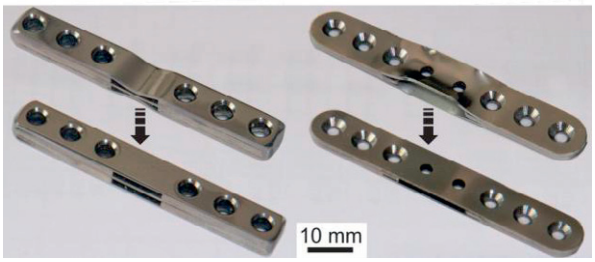

Fig. 6. NiTi-SMA implant samples. Triggering the one-way SME leads to a straightening of the outer NiTi sheets, hence altering the second moment of inertia within the middle part of the implant (left: increase, right: decrease).

In order to determine the effective alteration of the bending stiffness, based on the alteration of the second-moment of inertia, four-point-bending measurements were performed.

3.2. Determination of the bending stiffness

Four-point-bending tests showed a high variability of the alteration of the bending stiffness (Fig. 7) [9].

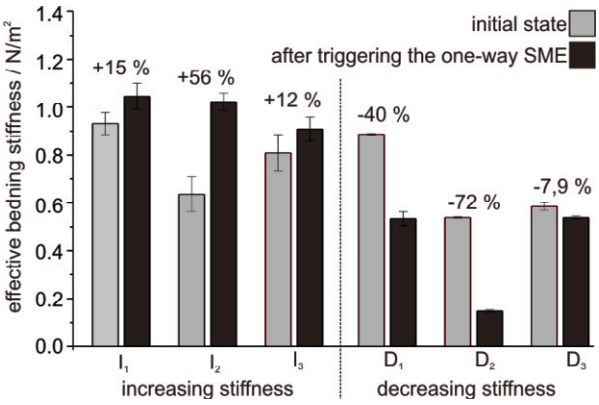

Fig. 7. Bending stiffness before (grey) and after (black) triggering the one-way-SME. Depending on the design (I_1-I_3 and D_1-D_3), both, an increase [9] or a decrease of the bending stiffness, induced by the one-way-SME can be achieved.

Depending on the design (i.e. height, width, geometry of the cross-section before and after triggering the one-way SME) an increase of the bending stiffness up to 56 % (Fig. 7, I_2) [9] and a decrease of the bending stiffness up to 72 % (Fig. 7, D_2) were determined.

It should be noted that the Young´s modulus of NiTi-SMAs is low compared to that of other orthopedic materials e.g. Ti (E = 105 GPa) or 316L (E = 210 GPa). This results in a lower bending stiffness compared to other implant materials, if the same dimensions are considered.

4. Outlook

This article gives a short overview on the possibility to use NiTi-SMA implants as stiffness alterable implantable osteosynthetic plates. Using an induction device, hence triggering the one-way-SME, the stiffness could be altered at an arbitrary date after implantation.

Currently, the implant dimensions are being increased in order to meet the requirements of a possible human application in terms of higher loads.

In order to pronounce the alteration of the bending stiffness, the use of locking screws is currently being investigated. As this would also increase the distance between bone and implant, the interaction between the actuator part (cf. Fig. 6) and the bone´s surface could be minimized.

Furthermore, the use of copper containing NiTi-SMAs offering lower transition temperatures and a narrow hysteresis are planned [29]. The utilization of this alloy would reduce the heat impact on the surrounding tissue during the induction process. This could expand this concept to further medical applications, e.g. compression, anchoring or expansion of SMA implants or devices. However, due to the high amount of copper, the biocompatibility as well as the mechanical and physical properties of this alloy have to be determined.

Acknowledgements

This work is funded by the “Deutsche Forschungsgemeinschaft (DFG)” (SFB 599, TPD10). The authors would like to thank the DFG for their support.

References

[1] Bartonicek, Jan., 2010. Early history of operative treatment of fractures. Arch Orthop Trauma Surg 130, p. 1385–1396.

[2] Bottlang, M., Lesser, M., Koerber, J., Doornink, J., von Rechenberg, B., Augat, P., Fitzpatrick, D. C., Madey, S. M., Marsh, J. L., 2010. Far cortical locking can improve healing of fractures stabilized with locking plates. J Bone Joint Surg Am. 92(7), p. 1652-1660.

[3] Döbele, S., Horn, C., Eichhorn, S., Buchholtz, A., Lenich, A., Burgkart, R., K. Nüssler, A., Lucke, M., Andermatt, D., Koch, R., Stöckle, U., 2010. The dynamic locking screw (DLS) can increase interfragmentary motion on the near cortex of locked plating constructs by reducing the axial stiffness. Langenbecks Arch Surg 395, p. 421–428.

[4] Claes, L. E., Wilke, H. J., Augat, P., Rubenacker, S., Margevicius, K. J., 2005. Effect of dynamization on gap healing of diaphyseal fractures under external fixation. Clin. Biomech. (Bristol, Avon) 10, p. 227-234.

[5] Pearson, O. M., Lieberman, D. E., 2004. The Aging ofWolffs „Law“: Ontogeny and Responses to Mechanical Loading in Cortical Bone. Yearbook of Physical Anthropology 47, p. 63-99.

[6] Pfeifer, R., Herzog, D., Hustedt, M., Barcikowski, S., 2010. Pulsed Nd:YAG laser cutting of NiTi shape memory alloys - Influence of process parameters. Journal of Materials Processing Technology 210, p. 1918-1925.

[7] Müller, C.W., Pfeifer, R., El-Kashef, T., Hurschler, C., Herzog, D., Oszwald, M., Haasper, C., Krettek, C., Gösling, T., 2010, Electromagnetic induction heating of an orthopaedic nickel--titanium shape memory device. J Orthop Res. 28(12), p. 1671-1676.

[8] Pfeifer, R., Hustedt, M., Wesling, V., Hurschler, C., Olender, G., Mach, M., Gösling, T., Müller, C.W., 2012. Noninvasive induction implant heating: An approach for contactless altering of mechanical properties of shape memory implants.Medical Engineering & Physics. In press. DOI: http://dx.doi.org/10.1016/j.medengphy.2012.03.010

[9] Olender, G., Pfeifer, R., Müller, C. W., Gösling, T., Barcikowski, S., Hurschler, C., 2011. A Preliminary Study of Bending Stiffness Alteration in Shape Changing Nitinol Plates for Fracture Fixation. Ann Biomed Eng. 39(5), p. 1546-4554.

[10] Kapanen, A., Ryhänen, J., Danilov, A., Tuukkanen, J., 2001. Effect of nickel-titanium shape memory metal alloy on bone formation. Biomaterials 22(18), p.2475-2480.

[11] Otsuka, K., Kakeshita, T., 2002. Science and technology of shape-memory alloys: new developments. MRS Bull. 27, p.91-100.

[12] Es-Souni, M., Es-Souni, M., Fischer-Brandies, H., 2005. Assessing the biocompatibility of NiTi shape memory alloys used for medical applications. Anal Bioanal Chem 381, p. 557-567.

[13] Feninat, F. E., Laroche, G., Fiset, M., Mantovani, D., 2001. Shape memory materials for biomedical applications. Adv Eng Mater 4, p. 91-104.

[14] Giroux, E. A., Maglione, M., Gueldry, A., Mantoux, J. L., 1996. Electromagnetic heating of a shape memory alloy translator. Appl Phys 29, p. 923-928.

[15] Gümpel. P., 2004. Formgedächtnislegierungen: Einsatzmöglichkeiten in Maschinenbau, Medizintechnik und Aktuatorik, Expert Verlag, Renningen.

[16] Pelton, A. R., Schroeder, V., Mitchell, M. R., Gong, X. Y., Barney, M., Robertson, S.W., 2008. Fatigue and durability of Nitinol stents. J. Mech. Behav. Biomed. Mater. 1, p. 153-164.

[17] Pelton, A.R., Stoeckel,D., Duerig, T.W., 2000. „Medical uses of nitinol”, Proceedings of the International Symposium on Shape Memory Materials 327-328, Kanazawa, Japan, p. 63–70.

[18] Peitsch, T., Klocke, A., Kahl-Nieke, B., Prymak, O., Epple, M., 2007. The release of nickel from orthodontic NiTi wires is increased by dynamic mechanical loading but not constrained by surface nitridation. J. Biomed. Mater. Res. A 82, p. 731-739.

[19] Tang, R.G., Dai, K.R., Chen, Y.Q., 1996. Application of a NiTi staple in the metatarsal osteotomy. Biomed Mater Eng 6, p. 307-312.

[20] Winkel, R., Marcus, O., Schlageter, M., Becker, M., 1999. NITINOL-Klammern zur Kompressionsosteosynthese des Kahnbeins. Trauma Berufskrankheiten, p. 182-186.

[21] Tarnita, D., Tarnita, D. N., Hacman, L., Copilus, C., Berceanu, C., 2012. In vitro experiment of the modular orthopedic plate based on Nitinol, used for human radius bone fractures. Rom. J. Morphol. Embryol. 5, p. 315-320.

[22] Domingo, S., Puértolas, S., Gracia-Villa, L., Mainar, M., Usónc, J., Puértolas, J. A., 2005. Design, manufacture and evaluation of a NiTi stent for colon obstruction Bio-Medical Materials and Engineering 15, p. 357-365.

[23] Huang, W., 1999. Modified shape memory alloy (SMA) model for SMA wire-based actuator design. J Intell Mater Syst Struct 10(3), p. 221-231.

[24] Brailovski, V., Prokoshkin, S. D., Khmelevskaya, I. Y., Inaekyan, K. E., Demers, V., Dobatkin, S.V. et al., 2006. Interrelations between the properties and structure of thermomechanically treated equiatomic Ti–Ni alloy. Mater Sci Eng A 438–440, p. 597-601.

[25] Lin, H.C., Lin, K.M., Chen, Y.C., 2000. A study on the machining characteristics of TiNi shape memory alloys. Journal of Materials Processing Technology 105, p. 327–332.

[26] Yung, K.C., Zhu, H.H., Yue, T.M., 2005. Theoretical and experimental study on the Kerf profile of the laser micro-cutting NiTi shape memory alloy using 355nm Nd:YAG. Smart Materials and Structures 14, p. 337–342.

[27] Haferkamp, H., Alvensleben, F., von Nolte, S., Kamlage, G., Paschko, S., 1999. Lasermaterialbearbeitung von Formgedächtnis-legierungen. LaserOpto 11, p. 58–62.

[28] Huang, H., Zheng, H.Y., Lim, D.C., 2004. Femtosecond laser machining characteristics of Nitinol. Applied Surface Sciences 228, p. 201–206.

[29] Zarnetta, R., Takahashi, R., L. Young, M., Savan, A., Furuya, Y., Thienhaus, S., Maaß, B., Rahim, M., Frenzel, J., Brunken, H., S. Chu, Y., Srivastava, V., D. James, R., Takeuchi, I., Eggeler, G., Ludwig, A., 2010. Identification of Quaternary Shape Memory Alloys with Near-Zero Thermal Hysteresis and Unprecedented Functional Stability. Adv. Funct. Mater. 20, p. 1917–1923.